MnBi thin films for high temperature permanent magnet applications

Cite as: AIP Advances **9**, 035325 (2019); https://doi.org/10.1063/1.5080004
Submitted: 05 November 2018 . Accepted: 11 January 2019 . Published Online: 15 March 2019

M. Villanueva, C. Navío, E. Céspedes, F. Mompeán, M. García-Hernández, J. Camarero, and A. Bollero

MnBi thin films for high temperature permanent magnet applications

Cite as: AIP Advances 9, 035325 (2019); doi: 10.1063/1.5080004
Presented: 17 January 2019 • Submitted: 5 November 2018 •
Accepted: 11 January 2019 • Published Online: 15 March 2019

M. Villanueva,[1,a)] C. Navío,[1] E. Céspedes,[1] F. Mompeán,[2] M. García-Hernández,[2] J. Camarero,[1,3] and A. Bollero[1]

AFFILIATIONS

[1] Division of Permanent Magnets and Applications, IMDEA Nanoscience, Madrid 28049, Spain
[2] Instituto de Ciencia de Materiales de Madrid, ICMM-CSIC, Madrid 28049, Spain
[3] Condensed Matter Physics Department, Autónoma University of Madrid (UAM), Madrid 28049, Spain

Note: This paper was presented at the 2019 Joint MMM-Intermag Conference.
[a)] **Corresponding author:** Melek Villanueva (melek.villanueva@imdea.org)

ABSTRACT

Thin films of ferromagnetic LTP-MnBi (Low Temperature Phase of MnBi) have been grown by magnetron sputtering onto quartz substrates. Two particular issues related to LTP-MnBi have been investigated: the strong influence of the growth temperature and the degradation of magnetic properties in time. The temperature dependence on the magnetic, morphological and microstructural properties has been investigated, evidencing drastic changes on the properties of MnBi with small temperature variations. By inducing a gradient of temperature during the growth, two well differentiated regions with different morphology and crystal structure have been observed in a MnBi film sample. On the other hand, aging experiments performed in a different LTP-MnBi sample has led to a notable decrease of 54% in the saturation magnetization after 6 days and a complete loss of ferromagnetic response after 4 months.

I. INTRODUCTION

In the last years, the scientific community has been making a great effort on developing new combinations of materials to overcome the problem on the scarcity of certain elements.[1,2] For this purpose, the use of the ferromagnetic manganese based alloys has been proposed for certain applications as rare earth free permanent magnets, magnetic recording media and spintronic devices.[3,4] Hard magnetic thin films with perpendicular magnetic anisotropy and high coercivity are attracting a lot of interest in spintronic devices and in MEMS (Magnetic Micromechanical Systems), including micro-motors, sensors and radiofrequency micro switches.[5–8]

LTP-MnBi is a ferromagnetic intermetallic compound which crystallizes in the NiAs-type hexagonal crystal structure. The interest in this alloy mainly comes from its large uniaxial magnetocrystalline anisotropy of 1.6 MJ/m^3 and a theoretical $(BH)_{max}$ of 17 MGOe. Moreover, the relatively high-Curie temperature of 711 K, which is limited by its phase transition to a paramagnetic high-temperature phase (HTP) at 630 K,[9] exceeds by 40 K to the Curie temperature of $Nd_2Fe_{14}B$.[10] In addition, the positive temperature coefficient of LTP-MnBi[11,12] makes it an interesting candidate for high temperature applications.

However, the MnBi system presents interesting anomalies that have not been completely understood. One of these anomalies is the strong dependence of magnetic properties and crystal structure with the applied temperature during LTP-MnBi formation. The other one is the degradation of magnetic properties with time. Recently, I. Janotová et al. have investigated the mechanism of LTP formation in MnBi based on thin ribbon flakes and they observed the degradation of the magnetic phase after exposure to ambient atmosphere, which was assigned to oxidation during one year time.[13] Also M. Y. Sun et al. observed significant influence of oxidation on structural and magnetic properties of LTP-MnBi thin films in absence of a capping layer.[14]

MnBi films were grown based on a prior study of the MnBi system prepared by sputtering.[15] It was observed that modifying the temperature during deposition and/or during post-growth annealing leads to different microstructures ranging from quasi-isotropic isolated MnBi micro-platelets to larger platelet-like individual ones

up to highly coalesced textured film-like areas. These microstructural variations determine the magnetic behavior, including the change in the easy axis direction and the possibility of varying coercivity from 4 to 16 kOe at room temperature.

In this work, we have focused on the reported anomalies of MnBi system. For that purpose, two types of MnBi films grown by magnetron sputtering have been analyzed. First, the type one of MnBi film (called MnBi-1) has been grown and subjected to a gradient temperature during LTP formation in order to analyze the temperature dependence on magnetic properties, morphology and crystal structure. Secondly, magnetic properties and crystal structure of a LTP-MnBi sample (called MnBi-2) have been studied over time in order to analyze aging effects.

II. EXPERIMENTAL

MnBi samples were grown by DC magnetron sputtering onto quartz substrates. The base pressure was about $3x10^{-8}$ mbar and the target to substrate distance was 75 mm. Prior to the growing of the films, the quartz substrates were ultrasonically treated and then heated up to 675 K for thermal cleaning in the sputtering chamber. A buffer layer of 50 nm of Bi was deposited into the quartz substrate followed by sequential deposition of Mn and Bi layers of 4 and 7 nm, respectively, and the number of layers, N, was fixed to 5. The sample was placed in direct contact with the surface of the heater and it was held in place by two Mo sample holding clips (one on each side of the sample). The temperature of the sample was measured using a K-type thermocouple. The temperature during the deposition (T_S) was 450 ± 50 K and after the deposition the temperature (T_A) was increased (575 ± 50 K) during 30 minutes to obtain the LTP-MnBi. Due to the experimental limitations, it was not possible to determine exactly the temperature on each side of the sample but as it will be shown in the following, only one side reached the LTP formation temperature. After cooling down to room temperature, a 10 nm capping layer of Ta was deposited on top of each sample to prevent from oxidation. Bi layers were sputtered from a Bi target (2", from Goodfellow, 99,9% purity) and Mn layers were obtained from a Mn target (2", from Goodfellow, 99,9% purity). Tantalum (Ta) capping layer was prepared using RF sputtering from a Ta target (2", from Kurt J. Lesker, 99,99% purity). Deposition started and ended with Bi to reduce the possible Mn oxidation. Deposition rates, obtained from a quartz balance, were 0.06 nm/s for Bi and 0.04 nm/s for Mn. Throughout the film growing procedure, the pressure in the chamber was maintained at $7.4x10^{-3}$ mbar.

M-H curves were obtained using a Vibrating Sample Magnetometer (VSM) with 20 kOe as the maximum applied field, both parallel (ip) and perpendicular (oop) to the film surface. Additionally, a superconducting quantum interference device (SQUID, Quantum Design MPMS) up to 50 kOe with a magnetic field applied both ip and oop to the film surface was used. All measurements were made at room temperature. The correction of the magnetization in emu/cm^3 was calculated from the sample area (obtained from sample total mass considering substrate density and thickness) and the total nominal thickness of the film.

Scanning electron microscopy (SEM) plane view micrographs were taken using a SEM-Auriga (Carl Zeiss, 30 kV) equipped with a field emission gun.

The crystal structure of the films was examined by X-ray diffraction (XRD) in θ-2θ geometry using Cu K_α radiation (λ = 0.1541 nm) using Bruker D8 T-T and X'Pert PRO Theta/2Theta Panalytical diffractometers. Thanks to the focused analysis region, it was possible to align independently the both sides of the sample. Further analysis of the Bragg peaks was performed in the SIDI crystallographic database (Universidad Autónoma de Madrid).

III. RESULTS AND DISCUSSION

In a previous work from our group[15] it was shown the dramatic change on the MnBi morphology attained within the growing parameters (mostly the temperature). It was shown that applying a growing temperature of 375 K, the microstructure of the sample presented a 3D-type growth, forming separated islands from 1 to 2 μm size. Moreover, XRD evidenced polycrystallinity. These uncoupled and small MnBi particles, slightly above the critical diameter for MnBi (about 0.5 μm in a spherical particle model),[6] elucidate the origin of the large coercivity obtained (16 kOe). On the other hand, applying a growing temperature of 450 K, the microstructure shows smooth crystalline and largely coalesced MnBi areas, with a well-defined (00l) orientation resulting in strong perpendicular magnetic anisotropy and a remarkable reduction of the coercive field from 16 to 4 kOe.[15] In a frame of magnetization reversal process based on nucleation and propagation of magnetic domains, the presence of isolated grains favors a nucleation-based inversion, explaining the large coercivity of the first sample explained. On the other hand, the increased particle size of the sample with smooth crystalline and largely coalesced MnBi areas can favor a domain wall propagation based inversion, explaining the change in coercive fields experimentally obtained.[15]

Based on these changes, a gradient sample was prepared in this work by modulation of the sample-heater thermal contact by exerting different pressure on the substrate edges. The total thickness of the sample was 50 nm of Bi buffer and 60 nm of MnBi, composed by 5 repetitions of Mn (7 nm) and Bi (4 nm) layers, ending with a 4 nm thick Bi layer. A Tantalum (Ta) capping layer was deposited at room temperature before the sample was exposed to air. It is fair to mention that during the post annealing process, where the formation of the LTP-MnBi is taking place, it is possible to observe, by visual inspection, a progressive change in the color of the sample: from soft grey to dark grey when the LTP-MnBi is obtained. In the case of the sample subjected to a gradient temperature, the change in the color was observed from the far right to the middle of the sample, so that the sample has two well differentiated regions with different colors and with a frontier wall located just in the middle of the sample (Fig. 1). The structures obtained on the right and left hand side of the sample (as shown in Fig. 1) correspond to a 3D-growth and to a smooth crystalline and largely coalesced MnBi areas, respectively, in good agreement with previous results.[15]

M-H curves and X-ray diffraction patterns of this sample (MnBi-1) are shown in Fig. 2. The VSM measurements have been made on the whole sample (without cutting it) and the overlapping of the magnetic signal of both sides of the sample can be observed. Only out of plane (oop) measurements are shown in M-H curves (Fig. 2–a) because the sample is isotropic.

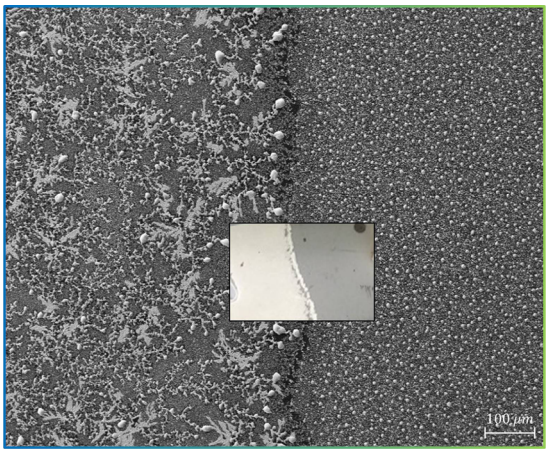

FIG. 1. SEM plane view of the center region of sample subjected to a gradient temperature MnBi-1. Inset shows top view of the sample. Shown sample dimensions: 4x8 mm^2.

The saturation magnetization of this sample is low (around 100 emu/cm^3) compared with the theoretical value (around 600 emu/cm^3) and two kinks are observed on the hysteresis loops: one around 2 kOe and the other one at 15 kOe. Two different X-ray diffraction measurements have been carried out (in the two halves of the sample) to compare the differences. The left side of the sample (Fig. 2–b, blue line) does not show intensity peaks from MnBi alloy, except a small presence of LTP-MnBi phase (Ref: 04-004-7897). The higher peak corresponds to metallic Bi (Ref: 00-001-0699) and the other peaks are a combination of metallic Bi, manganese oxide (Ref: 04-006-8109) and it can be even observed a non-negligible peak of $Mn_3O_8Ta_2$ (Ref: 01-089-5524) very likely coming from the oxidation of the capping layer which will be analyzed later. This contribution was observed as well by Chunhong Li et al[16] in as-cast MnBi ingot obtained via arc melting. In addition, J. Cao et al[17] have shown a complicated intergranular phase containing Mn, Bi, and MnO phases in addition to an amorphous phase in MnBi magnets prepared by spark plasma sintering using ball milling powders as precursors without purification.

On the right side of the sample (green line from Fig. 2–b) the intensity of the main peak of metallic Bi has decreased and some little diffraction peaks from metallic Bi have disappeared. In this side of the sample, the main peak from LTP-MnBi is much prominent than in the other side. These differences between the two halves of the sample could explain the two magnetic contributions (different reversal fields) observed in the M-H curves shown in Fig. 2–a. The first transition around 2 kOe is assigned to reversal of the left side of the sample because of the high presence of dendrite-type morphology favoring a domain wall propagation based inversion. On the other hand, the second transition around 15 kOe can be assigned to the right side of the sample, due to the presence of clearly isolated features, favoring a nucleation-based inversion. From the XRD studies we conclude that there is a big amount of Mn and Bi, which has not been alloyed, in agreement with the low magnetization in the M-H curves (around 110 emu/cm^3).

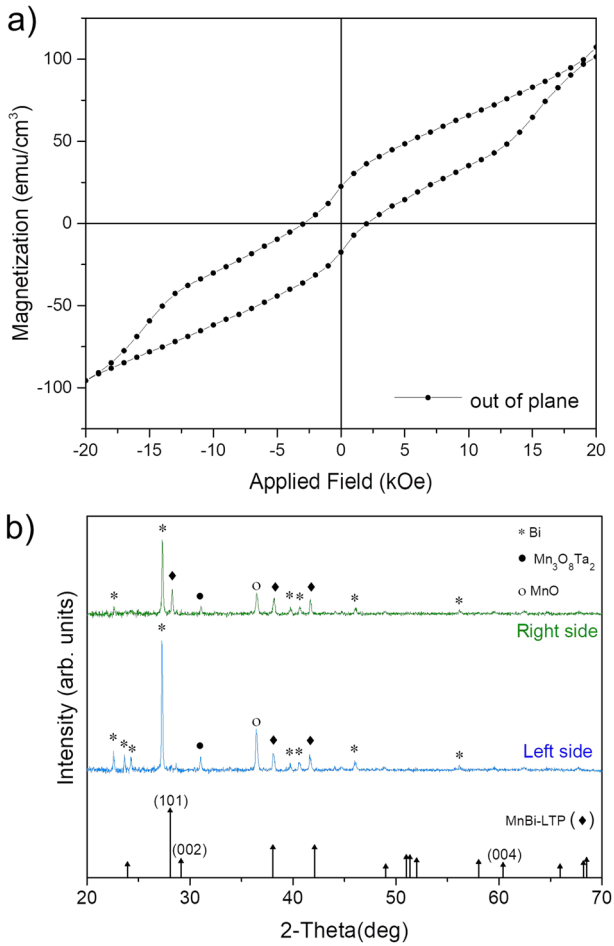

FIG. 2. a) M-H curve of MnBi sample subjected to a gradient temperature (MnBi-1) b) XRD diffraction patterns of the two regions of the sample. Green line (right side of the sample in Fig. 1) corresponds to the region subjected to higher temperature and blue line (left side of the sample in Fig. 1) corresponds to the lower temperature one.

Somehow, the thermal gradient has considerably affected the Mn-Bi alloy formation and consequently, the ferromagnetic MnBi phase.

The big amount of non-alloyed peaks such as metallic Mn and Bi attached to the presence of a Mn oxide peak and, most important, the $Mn_3O_8Ta_2$ peak can be related to the degradation of MnBi samples with time, which is one of the challenges of the LTP-MnBi.[13,14] It is well known that Mn oxidizes more easily than Bi so an ending Bi layer with a higher nominal thickness or a different capping layer could be a solution to the oxidation problem. Nevertheless, it has been recently reported by Quarterman et al.[18] that, depending on the material chosen as a capping layer, coercivity or magnetization saturation can be developed, as well as magnetic properties can completely disappear. They concluded that a capping layer of Ta could enhance the magnetization, a capping layer of SiO_2 could enhance the coercive field and capping layers of Au and Cr do not allow the formation of LTP-MnBi.

The second investigated sample (MnBi-2), was prepared with T_S = 400 K, T_A = 625 K and covered with 10 nm Ta capping. This film has been used for an aging study of LTP-MnBi and a fast degradation with time has been observed. As it can be seen in Fig. 3–a, a decrease of 54% of the saturation magnetization has been produced after 6 days (orange dotted line) and, after 4 months, the ferromagnetic response of the sample has almost vanished (purple triangles line).

XRD patterns of this sample after growth (before degradation) are shown in Fig. 3–b, evidencing both LTP-MnBi phase and a metallic Bi contribution. The huge amount of metallic Bi is not surprising due to the 50 nm Bi buffer. It is remarkable that not all the LTP-MnBi Bragg peaks appear, showing preferential growth in the perpendicular direction of the film plane, being the (002) MnBi Bragg peak the most intense one and showing a non-negligible contribution from (004) peak. This agrees with the c-axis preferential alignment of the hexagonal LTP-MnBi phase.

XRD measurements have been carried out after 4 months, when the sample is almost completely degraded. According to that, it can be seen that all the LTP-MnBi Bragg peaks have vanished and the only remaining Bragg peaks are the ones corresponding to metallic Bismuth.

This could be because the thickness of the protective layer was not thick enough to completely protect the microstructured films. In the case of non-continuous films or particulated morphologies, degradation might be a particular issue despite the capping layer on top, since oxidation might emerge from uneven coating or partial covering of the edges.

The result is in good agreement with previous studies focused on bulk MnBi samples, evidencing the rapid oxidation of this material and its key role on the magnetic properties of this system.

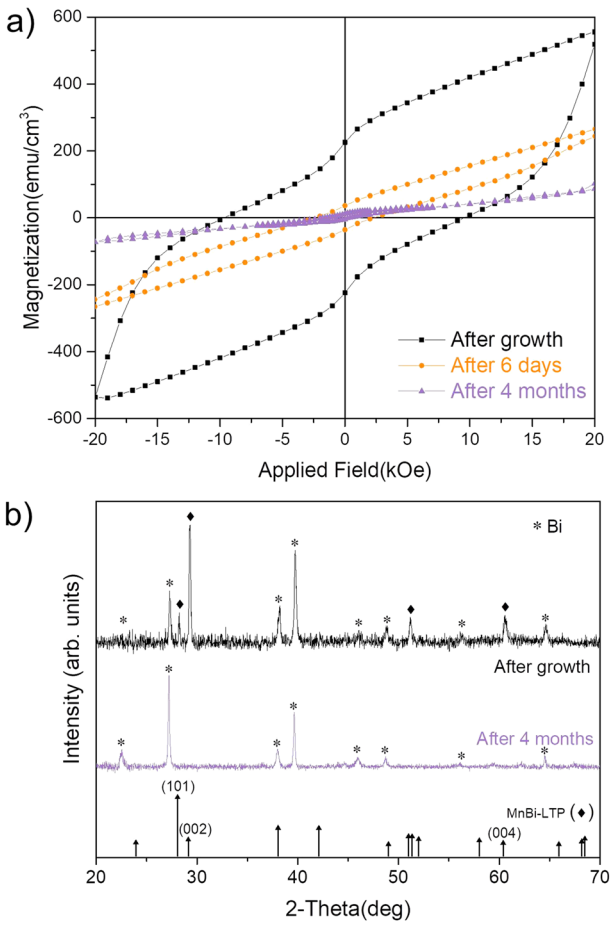

FIG. 3. a) Out of plane M-H curves of MnBi-2 sample after growth (black squares), after 6 days (orange dots) and after 4 months (purple triangles), b) XRD diffraction patterns before and after degradation.

IV. CONCLUSIONS

Two studies have been performed to understand the influence of temperature and time with the purpose of further understanding of MnBi anomalies.

Based on a previous research,[15] where a deep study on how temperature -before and after growth- affects the properties of MnBi films, we have observed two different morphologies and microstructures formed during the growth process on a MnBi gradient-sample with two well-differentiated regions. Island- and dendritic-type structures are obtained with increasing the post-annealing temperature. The differences have been well correlated with magnetic properties and with XRD data. Two different magnetic contributions have been observed in the M-H curves. The lower and higher field reversal corresponds to the dendritic- and island-type MnBi regions, respectively. The different magnetic behavior is in good agreement with XRD measurements done on each region of the gradient sample. Moreover, the whole sample shows Bragg peaks corresponding to metallic Bi, metallic Mn, and Mn compounds such as $Mn_3O_8Ta_2$. These secondary phases are not easily found in MnBi compounds.

Time dependence on magnetic properties and crystal structure were also studied. It is found that after 4 months the ferromagnetic response completely disappears, in agreement with a significant change of the crystal structure leading to LTP-MnBi disappearance.

Considering both, XRD and the M-H analysis, it can be concluded that the formation of pure crystalline LTP-MnBi is strongly dependent on the uniformity of the annealing process. For these samples, either a thicker Ta capping or a combination of two capping layers would be needed in order to maintain the magnetic and structural properties of the LTP-MnBi films.

ACKNOWLEDGMENTS

The authors acknowledge the financial support from the Spanish Ministerio de Economía y Competitividad (MINECO) through NEXMAG (M-era.Net Programme, Ref. No. PCIN-2015-126), 3D-MAGNETOH (Ref. No. MAT2017-89960-R) and Ref. No. MAT2014-52402-C2-2-R, and from the Regional Government of Madrid through NANOMAGCOST project (Ref. P2018/NMT-4321).

REFERENCES

[1]J. Cui, M. Kramer, L. Zhou, F. Liu, A. Gabay, G. Hadjipanayis, B. Balasubramanian, and D. Sellmyer, Acta Materialia **158**, 118 (2018).

[2]K. Patel, J. Zhang, and S. Ren, Nanoscale **10**, 11701 (2018).

[3]A. Kalache, S. Selle, W. Schnelle, G. H. Fecher, T. Höche, C. Felser, and A. Markou, Physical Review Materials **2**(8), 084407 (2018).

[4]H. Wu, I. Sudoh, J. Kim, G. Vallejo-Fernandez, and A. Hirohata, *Magnetics Conference (INTERMAG), 2017 IEEE International*. IEEE, pp. 1–1, 2017.

[5]M. Gibbs, E. Hill, and P. Wright, Journal of Physics D: Applied Physics **37**(22), R237 (2004).

[6]T. Hozumi, P. LeClair, G. Mankey, C. Mewes, H. Sepehri-Amin, K. Hono, and T. Suzuki, Journal of Applied Physics **115**(17), 17A737 (2014).

[7]J. Rial, M. Villanueva, E. Céspedes, N. López, J. Camarero, L. Marshall, L. Lewis, and A. Bollero, Journal of Physics D: Applied Physics **50**(10), 105004 (2017).

[8]C. Navío, M. Villanueva, E. Céspedes, F. Mompeán, M. García-Hernández, J. Camarero, and A. Bollero, APL Materials **6**, 101109 (2018).

[9]X. Jiang, T. Roosendaal, X. Lu, O. Palasyuk, K. W. Dennis, M. Dahl, J.-P. Choi, E. Polikarpov, M. Marinescu, and J. Cui, Journal of Applied Physics **119**(3), 033903 (2016).

[10]A. Andreev, A. Deryagin, N. Kudrevatykh, N. Mushnikov, V. Reimer, and S. Terent'ev, Sov. Phys.-JETP (Engl. Transl.) **63**(3), 608 (1986).

[11]V. Ly, X. Wu, L. Smillie, T. Shoji, A. Kato, A. Manabe, and K. Suzuki, Journal of Alloys and Compounds **615**, S285 (2014).

[12]J. Cui, J.-P. Choi, G. Li, E. Polikarpov, J. Darsell, N. Overman, M. Olszta, D. Schreiber, M. Bowden, T. Droubay, M. J. Kramer, N. A. Zarkevich, L. L. Wang, D. D. Johnson, M. Marinescu, I. Takeuchi, Q. Z. Huang, H. Wu, H. Reeve, N. V. Vuong, and J. P. Liu, Journal of Physics: Condensed Matter **26**(6), 064212 (2014).

[13]I. Janotová, P. Švec, I. Mat'ko, D. Janickovic, and P. Švec, Sr., AIP Conference Proceedings **1996**(1), 020021 (2018).

[14]M. Sun, X. Xu, X. Liang, X. Sun, and Y. Zheng, Journal of Alloys and Compounds **672**, 59 (2016).

[15]E. Céspedes, M. Villanueva, C. Navío, F. Mompeán, M. Garcá-Hernández, A. Inchausti, P. Pedraz, M. Osorio, J. Camarero, and A. Bollero, Journal of Alloys and Compounds **729**, 1156 (2017).

[16]C. Li, D. Guo, B. Shao, K. Li, B. Li, and D. Chen, Materials Research Express **5**(1), 016104 (2018).

[17]J. Cao, Y. Huang, Y. Hou, G. Zhang, Z. Shi, Z. Zhong, and Z. Liu, AIP Advances **8**(5), 055132 (2018).

[18]P. Quarterman, D. Zhang, K. B. Schliep, T. J. Peterson, Y. Lv, and J.-P. Wang, Journal of Applied Physics **122**(21), 213904 (2017).